ADVANCES IN ATMOSPHERIC SCIENCES, VOL. 34, JULY 2017, 877–893

• **Original Paper** •

Comparison of Aerosol Effects on Simulated Spring and Summer Hailstorm Clouds

Huiling YANG*[1], Hui XIAO[1,3], Chunwei GUO[2], Guang WEN[1], Qi TANG[1], and Yue SUN[1,3]

[1]*Key Laboratory of Cloud Precipitation Physics and Severe Storms, and Center of Disaster Reduction, Institute of Atmospheric Physics, Chinese Academy of Sciences, Beijing* 100029*, China*

[2]*Environmental Meteorology Forecast Center of Beijing–Tianjin–Hebei, Beijing* 100089*, China*

[3]*University of Chinese Academy of Sciences, Beijing* 100049*, China*

(Received31 May 2016; revised 8 February 2017; accepted 17 March 2017)

ABSTRACT

Numerical simulations are carried out to investigate the effect of cloud condensation nuclei (CCN) concentrations on microphysical processes and precipitation characteristics of hailstorms. Two hailstorm cases are simulated, a spring case and a summer case, in a semiarid region of northern China, with the Regional Atmospheric Modeling System. The results are used to investigate the differences and similarities of the CCN effects between spring and summer hailstorms. The similarities are: (1) The total hydrometeor mixing ratio decreases, while the total ice-phase mixing ratio enhances, with increasing CCN concentration; (2) Enhancement of the CCN concentration results in the production of a greater amount of small-sized hydrometeor particles, but a lessening of large-sized hydrometeor particles; (3) As the CCN concentration increases, the supercooled cloud water and rainwater make a lesser contribution to hail, while the ice-phase hydrometeors take on active roles in the growth of hail; (4) When the CCN concentration increases, the amount of total precipitation lessens, while the role played by liquid-phase rainfall in the amount of total precipitation reduces, relatively, compared to that of ice-phase precipitation. The differences between the two storms include: (1) An increase in the CCN concentration tends to reduce pristine ice mixing ratios in the spring case but enhance them in the summer case; (2) Ice-phase hydrometeor particles contribute more to hail growth in the spring case, while liquid water contributes more in the summer case; (3) An increase in the CCN concentration has different effects on surface hail precipitation in different seasons.

Key words: cloud condensation nuclei (CCN), microphysical process, hailstorm, precipitation

Citation: Yang, H. L., H. Xiao, C. W. Guo, G. Wen, Q. Tang, and Y. Sun, 2017: Comparison of aerosol effects on simulated spring and summer hailstorm clouds. *Adv. Atmos. Sci.*, **34**(7), 877–893, doi: 10.1007/s00376-017-6138-y.

1. Introduction

Hailstorms often cause fiercely disastrous weather involving hail, heavy rain, gales, and lightning (Khain et al., 2004; Lynn et al., 2005). In China, hail events are one of the most extreme weather phenomena and every year give rise to considerable adverse human impacts. Aerosol particles can act as cloud condensational nuclei (CCN) and may dramatically influence the cloud microphysical processes of strong convective clouds, and then impact their microphysical structure and the distribution of precipitation (Feingold et al., 1999; Yin et al., 2000a, 2000b; Saleeby and Cotton, 2004; Rosenfeld et al., 2006; Flossmann and Wobrock, 2010; Chen et al., 2011b; Xiao et al., 2014).

Sizes and concentrations of cloud droplets and ice crystals may be significantly affected by CCN concentrations (Chen and Xiao, 2010). Many studies have verified that high concentrations of aerosols can form a large number of smaller cloud droplets and cause a slowing of the coalescence process of cloud droplets (Squires and Twomey, 1961; Xiao et al., 1988; Kaufman and Nakajima, 1993; Rosenfeld and Lensky, 1998; Andreae et al., 2004). The numerous cloud droplets produced by CCN from aerosols can ascend to higher altitudes of the atmosphere and then freeze into ice precipitating particles in deeper convective clouds. (Phillips et al., 2002; Rosenfeld et al., 2008). The release of latent heat due to freezing at higher altitudes further invigorates updrafts and leads to the formation and development of deeper clouds. When the frozen-ice precipitating particles reach the lower altitudes of the atmosphere, they melt and consume a large quantity of latent heat, thus accelerating low-level downdrafts that can initiate new storms (Seigel and van den Heever, 2013).

As noted by Saleeby et al. (2009), the formation rate of ice crystals may also be significantly affected by the CCN

* Corresponding author: Huiling YANG
Email: yanghuiling@mail.iap.ac.cn

concentration. They found that aerosols acting as CCN can influence cloud droplet number concentrations and droplet sizes. The cloud droplets can ascend to high altitudes in convective clouds, and then the droplet size changes can impact ice particle riming efficiencies (Hindman et al., 1994). These efficiencies decrease with reduced cloud droplet diameter (Pitter and Pruppacher, 1974). The cloud droplet diameter decreases as the CCN concentration enhances, and therefore the ice crystal riming efficiencies also decrease with increasing CCN concentration (Pitter and Pruppacher, 1974; Saleeby et al., 2009). Khain et al. (2001) found that, in polluted clouds, the conversion of cloud droplets to ice particles is inefficient until a level of homogeneous freezing is reached. This result agrees with aircraft measurements showing evidence of sustained supercooled liquid water down to −38°C in continental mixed-phase convective clouds (Rosenfeld, 2000; Rosenfeld et al., 2006). Large numbers of cloud droplets with smaller diameters form with increasing CCN concentration, and the formation efficiency of ice particles is reduced with an enhancement in small-sized droplets (Borys et al., 2000; Wang and Ji, 2000), which may be one reason for the presence of sustained super-cooled liquid water down to −38°C. Recently, Shi et al. (2015) found that ice mass flux enhancement in continental thunderclouds results in stronger lighting production.

The aerosol effects on the precipitation of convective clouds are sensitive to cloud microphysical and dynamical properties (Khain et al., 1999). An increase in the concentration of aerosols can lead to either an enhancement or a suppression of precipitation (Seifert and Beheng, 2006; Cheng et al., 2009). Seifert et al. (2012) found that the variation in CCN has a significant effect on cloud microphysical properties, such as the amounts of cloud water condensate, snow and rain, as well as on the glaciation of the clouds, but the effects on surface precipitation are small. Khain et al. (2004) found that both the precipitation rate and the precipitation amount depend crucially on the CCN concentration. However, some other studies have shown precipitation enhancement around heavily polluted urban areas (Ohashi and Kida, 2002; Shepherd and Burian, 2003).

The latent heat released during the freezing of supercooled liquid water feeds back in an important way to the microphysical and dynamical processes of convective clouds (Guo et al., 2006a, 2006b, 2014; Xiao et al., 2016). Khain et al. (2004) found that aerosols affect the vertical profile of the convective heating caused by latent heat release. Koren et al. (2005) examined microphysical properties derived from MODIS and found that aerosols can invigorate convective clouds over the Atlantic Ocean. Teller and Levin (2006) found that, in a moist and unstable atmosphere, pollution aerosols can induce clouds to develop stronger updrafts and downdrafts, grow taller, trigger secondary storm development, and produce more rain.

Aerosol particles can also act as giant CCN (GCCN; > 1 μm in radius) and ice nuclei (IN) affecting cloud microphysical properties and precipitation (Mather, 1991; Kaufman et al., 2005; Lin et al., 2006). Aerosols, primarily those with compositions to act as CCN, entering the hailstorm cloud, can influence the resulting cloud droplet number concentration and droplet size. The change in cloud droplet size impacts ice particle riming efficiencies. The "aerosol indirect effect" (Twomey, 1977; Albrecht, 1989) is the hypothesis that an increase in pollution aerosols leads to an increase in CCN, an increase in cloud droplet number concentrations and, consequently, suppression of precipitation, in any liquid-phase cloud system. Mixed-phase hailstorm clouds are also sensitive to the degree of pollution aerosols. The present study focuses on the CCN effects on hailstorms.

The simulation of hail formation in severe storms is an important problem in cloud physics (Liu and Niu, 2009; Yang et al., 2015a, 2015b). Freezing precipitation is an extremely hazardous form of weather (Chen et al., 2011a; Guo et al., 2015), with hailstorms posing serious economic threats in many places around the world. The effect of aerosols on clouds and precipitation is seen as a major scientific challenge in climate modeling (IPCC, 2007), and such challenges in terms of studying the effects of aerosols on the cloud microphysical properties and precipitation of hailstorms still exist. For example, the impacts of aerosols on convective clouds vary seasonally and regionally (Khain et al., 2005; Yin et al., 2005). Although previous studies have shown that aerosols can affect the development of convective clouds, the interactions between aerosols and ice particles are still poorly understood. Very little attention has been paid to how aerosols influence the microphysical characteristics in hailstorm clouds. The impacts of aerosols on ice-phase precipitation are difficult to estimate (Khain et al., 2004; Zhao et al., 2005) because their influence changes both temporally and spatially. However, we can, based on the results of model simulations, estimate the impacts of aerosols on ice-phase precipitation for a particular cloud system. We hope that the conclusions obtained from the storms studied in the present work will hold some relevance, and can be applied, globally.

Because the atmospheric stratification differs for the formation of hail clouds between spring and summer (in particular, the 0°C height is different), the thickness of the warm layer and the supercooled layer also differs during the development of clouds in these two seasons. Examining the similarities and differences of the effects of CCN on the cloud microphysical processes and distribution of precipitation for hail clouds between spring and summer in the same region carries great scientific significance and application value, particularly for the fields of severe weather forecasting and weather modification. However, these issues have not yet been the subject of in-depth study.

Previous studies on the effects of aerosols on the macro- and microphysical processes of hail clouds have mostly focused on the same season, such as summer (Khain et al., 1999; Seifert and Beheng, 2006; Shi et al., 2015); studies comparing the effects between seasons are rarely seen in the literature. This is the gap addressed in the present study. At the same time, from those previous single-season studies, it is clear that CCN number concentrations in polluted clouds are generally less than 2000 cm^{-3}. For example, 1000 cm^{-3}

(Khain et al., 1999; Cheng et al., 2009), 1350 cm^{-3} (Teller and Levin, 2006) and 1900 cm^{-3} (Saleeby et al., 2009) are quantities separately reported in different studies before. Air pollution is very serious in China, with CCN number concentrations sometimes reaching 5000 cm^{-3}, and the effects of aerosols on hailstorm clouds might be more complicated in such seriously polluted conditions.

The goal of the present study is to characterize and compare the properties of aerosol effects on hailstorm clouds in different seasons in Northeast China. The similarities and differences of the effects of CCN on cloud microphysical and precipitation processes between hail clouds in spring and summer are investigated to provide meaningful conclusions regarding the impact of air pollution on hailstorms. Particular effort is made to investigate the interactions between aerosols and ice particles. The impacts of aerosols on ice-phase precipitation are also considered. The setup of the numerical model used to conduct the simulations and the experimental design are discussed in section 2. A comparison of radar echo, precipitation and the pressure field is presented in section 3. The results of the numerical experiments are described and discussed in section 4. And finally, a summary of our findings, along with our conclusions, is provided in section 5.

2. Model description

The model chosen for this study is the improved Regional Atmospheric Modeling System (RAMS; Saleeby and Cotton, 2004, 2005). All simulations are run in the same model domain. A detailed description of the model can be found in Yang et al. (2011). RAMS is configured on an Arakawa-C grid and sigma-z terrain-following coordinate system. CCN and GCCN collectively as "aerosol particles", and their concentrations as the "aerosol concentrations". The aerosol concentrations have a lognormal size distribution, with a median radius of 0.04 and 3 μm for CCN and GCCN, respectively. Activations of CCN, GCCN and IN are simulated based on Saleeby and Cotton (2004). RAMS predicts two moments (mixing ratio and number concentration) of hydrometeor distributions for rain, pristine ice, snow, aggregates, graupel and hail (Meyers et al., 1997; Cotton et al., 2003). The two-moment approach is used for the cloud droplet distribution via a parameterization for the formation of cloud droplets from activation of CCN within a lifted parcel (Saleeby and Cotton, 2004). The cloud droplet spectrum is divided into two sections: cloud droplets from 1 to 40 μm in diameter, taken as small cloud droplets (c1); and cloud droplets from 40 to 80 μm in diameter, named large cloud droplets (c2). These two modes of cloud droplets are independently nucleated via activation of CCN and GCCN by using the look-up tables derived from a Lagrangian model (Feingold et al., 1994). IN are activated according to the formula developed by Meyers et al. (1992). According to this formula, ice crystals are nucleated from IN as a function of supersaturation with respect to ice.

In RAMS, cloud droplets and rain are liquid water, but may be supercooled. The mean size of cloud droplets is not allowed to grow beyond 80 μm, while the mean size of rain is not allowed to become less than 80 μm. Cloud droplets are assumed small enough to not fall, while all other categories do fall. Cloud droplets and pristine ice are the only categories to nucleate from vapor. All other categories are from the existing hydrometeors but, once formed, may also grow by vapor deposition. Pristine ice, snow and aggregates are assumed to be completely frozen. The definition of the pristine ice category is restricted to relatively small crystals that nucleate from vapor, and larger pristine ice crystals are categorized as snow. The main distinction between pristine ice crystals and snow is the size of the crystals. The mean size of pristine ice is not allowed to grow beyond 100 μm, while the mean size of snow is not allowed to become less than 100 μm. The snow category is defined here as consisting of relatively large ice crystals that have grown by vapor deposition and riming. Together, the pristine ice and snow categories allow a bimodal representation of ice crystals. During conditions of ice supersaturation, the pristine ice number concentration and mass mixing ratio are transferred to the snow category by vapor deposition growth (Harrington et al., 1995). Aggregates are defined as ice crystals that have formed by collision and coalescence of pristine ice, snow and other aggregates. Graupel and hail are mixed-phase categories, capable of consisting of ice only or a mixture of ice and liquid. Graupel is an intermediate density hydrometeor, is assumed to be approximately spherical in shape, and to be formed by moderate to heavy riming and partial melting of pristine ice, snow and aggregates. Graupel is allowed to carry up to only a low percentage ($< 30\%$) of liquid. If the percentage becomes larger, by either melting or riming, a graupel particle is re-categorized as hail. Hail is a high-density hydrometeor, considered to be spherical in shape. It is assumed to be formed by the freezing of rain drops or by the riming or partial melting of graupel. Hail is allowed to carry any fraction of liquid water (except 100%). The definitions of graupel and hail emphasize their composition and density more than their method of formation.

CCN concentrations are homogeneous horizontally, with a vertical profile that decreases linearly with height up to 4 km above ground level, and then has a constant concentration of 100 cm^{-3} above 4 km. The CCN distribution follows some in-situ observations (van den Heever et al., 2006; Shi and Duan, 2007; Duan et al., 2008). The initial CCN concentrations at the surface are assumed to be 300 cm^{-3} (C1, clean case), 1000 cm^{-3} (C2, polluted case), and 5000 cm^{-3} (C3, heavily polluted case). The initial background IN and GCCN concentration are the same as in previous study (van den Heever et al., 2006).

Two-way nesting with a three-domain arrangement is used (Fig. 1). The outer domain, domain-1 (G1), covers most of northern China, with a 10-km grid-spacing resolution and 160 (lon) × 200 (lat) grid points; domain-2 (G2) covers the central eastern region of Inner Mongolia, and northern Hebei and Shanxi provinces in northern China, with a 2.5-km grid-spacing resolution and 250 (lon) × 242 (lat) grid points; and domain-3 (G3) surrounds the major hailfall area, with a 500-m grid-spacing resolution and 227 (lon) × 215 (lat) grid

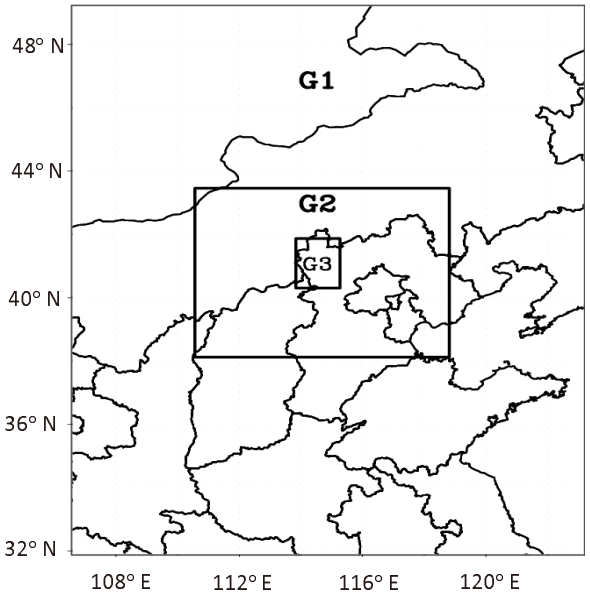

Fig. 1. The modeling regions: domain-1 (G1); domain-2 (G2); domain-3 (G3).

points. Within each domain there are 42 vertical levels, with a minimum grid spacing of 75 m near the surface. A vertical grid stretching, with a stretch ratio of 1.1 and a maximum vertical grid spacing of 750 m, is used in the model simulation. The Kain–Fritsch cumulus parameterization scheme is used in domain-1, and the convection is explicitly resolved both in domain-2 and domain-3.

Two hailstorm cases are used to examine the impact of aerosols on deep, precipitating weather systems occurring in two different seasons over the same area. One occurred in spring over a semi-arid area in northern Hebei Province in northern China on 23 April 2009 (referred to as the SPR hailstorm), and the other occurred in summer in the same area on 23 July 2009 (referred to as the SUM hailstorm). The SPR hailstorm case has been well studied previously (Yang et al., 2011, 2012).

The SPR and SUM simulations are triggered at 0000 UTC 23 April 2009 and 0000 UTC 23 July 2009, respectively, and run for 18 h. The meteorological data for the initial conditions and boundary fields of the simulations are all from NCEP $1^\circ \times 1^\circ$ 6-h data. The hailfall of the SPR case occurred between 0550 UTC and 0930 UTC 23 April 2009, and covered most of area A [the red rectangular area marked in Fig. 2b (40.7°–41.5°N, 114.3°–115.8°E)]; and the hail precipitation of the SUM case occurred between 0520 UTC and 0930 UTC 23 July 2009, and covered most of area B [the red rectangular area marked in Fig. 2d (40.4°–41.6°N, 114°–116°E)].

3. Comparison of the simulations to observations

This study focuses on investigating the microphysical properties and precipitation response to CCN number variations. Comparing the simulated and observed results provides a general assessment of the ability of the model for further use in this study.

For the SPR case, there was a deeply developed cold vortex cloud system maintained over eastern Inner Mongolia at 0500 UTC 23 April 2009. The study region was located at the tail of this cloud system. At first, many small-scale convective cloud clusters occurred in the cloud system; and then, these small-scale convective cells moved from the southwest to the northeast and merged into strong convective systems, resulting in a large area of hailfall in the region. Figures 2a and b compare the 6-h accumulated rainfall amounts of the observed and simulated SPR case. From the figures, we can see that the distributions of the accumulated rainfall amount between the simulation and observation are very similar. A detailed account of the simulations and observations for the SPR case has already been published (Yang et al., 2011), and so will not be presented here in this paper.

For the SUM case, there was a high-altitude trough line at 0500 UTC 23 July 2009 over the study region. Northwesterly wind prevailed behind the trough line, and cold air moved downwards along this northwesterly wind. The pressure was low and the temperature was high near the surface. The upper-level cold air met with the low-level warm air, and a ground convergence line was formed. Many small-scale convective cells occurred and moved from northwest to southeast, merging into strong convective clouds and resulting in hail weather in this area. The results from the simulations and observations for the SUM case are illustrated in Figs. 2c–h. The pattern of simulated 6-h accumulated precipitation agrees well with the radar observations, with the maximum precipitation for both simulations and observations being approximately 20 mm (Figs. 2e and f). The shape and location of the simulated pressure is also similar to those observed (Figs. 2c and d). Figures 2g and h depict a general comparison of the radar reflectivity between the simulated and observational results. The simulated radar reflectivity distributions at 0630 UTC are consistent with those observed, in shape and trend, and the maximum radar reflectivity for both is the same, at about 50 dBZ. The radar reflectivity figure concerns the development stage of convective cloud, while the precipitation figure relates to the 6-h accumulated rainfall. Therefore, the location of maximum precipitation does not correspond to the location of maximum radar reflectivity.

Overall, the simulations are in accordance with the observations, indicating the simulation results—both for the SPR case and the SUM case—are trustworthy and accurate.

4. Model results

4.1. *Influences of CCN on the horizontal distribution of hydrometeor particles*

Figures 3 and 4 present the vertically integrated (vint) hydrometeor mixing ratio and ice-phase mixing ratio for the SPR and SUM cases, respectively. The vertical integration

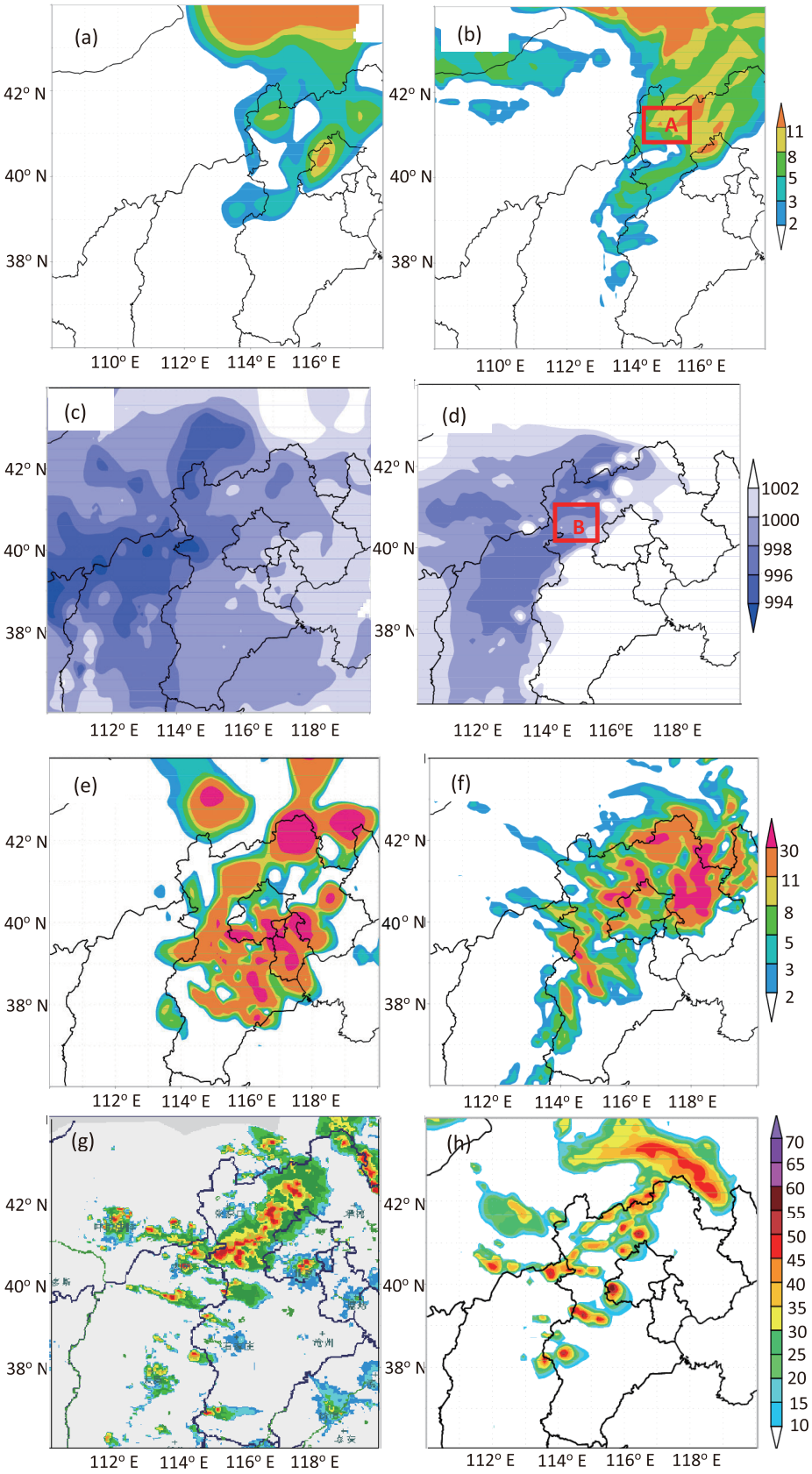

Fig. 2. (a, b) Comparison of the (a) observed and (b) simulated 6-h (0600–1200 UTC) accumulated rainfall amount (units: mm) of the SPR case. (c–h) Comparison of the (c, e, g) observed and (d, f, h) simulated (c, d) 0600 UTC sea level pressure (units: hPa), (e, f) 6-h (0600–1200 UTC) accumulated rainfall amount (units: mm), and (g, h) 0630 UTC radar echoes, of the SUM case. The red rectangular areas A and B represent the hail precipitation area for SPR case and SUM case, respectively.

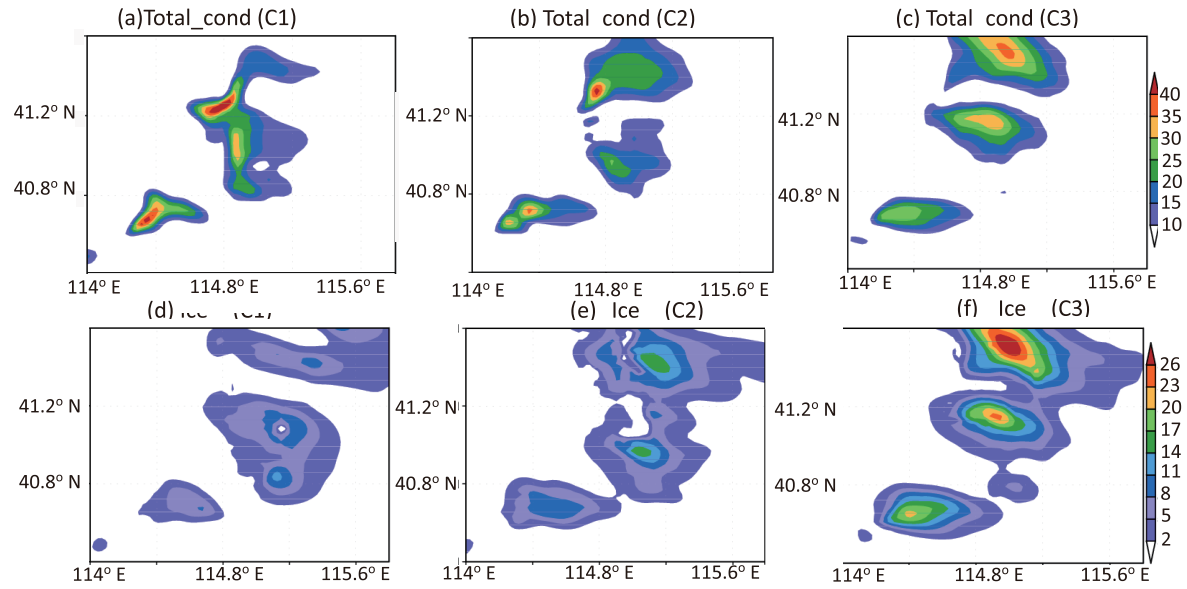

Fig. 3. Vertically integrated condensate mixing ratio and ice mixing ratio at 0700 UTC 23 April 2009 (SPR) for the three experiments (C1, C2, C3) (units: g kg^{-1}).

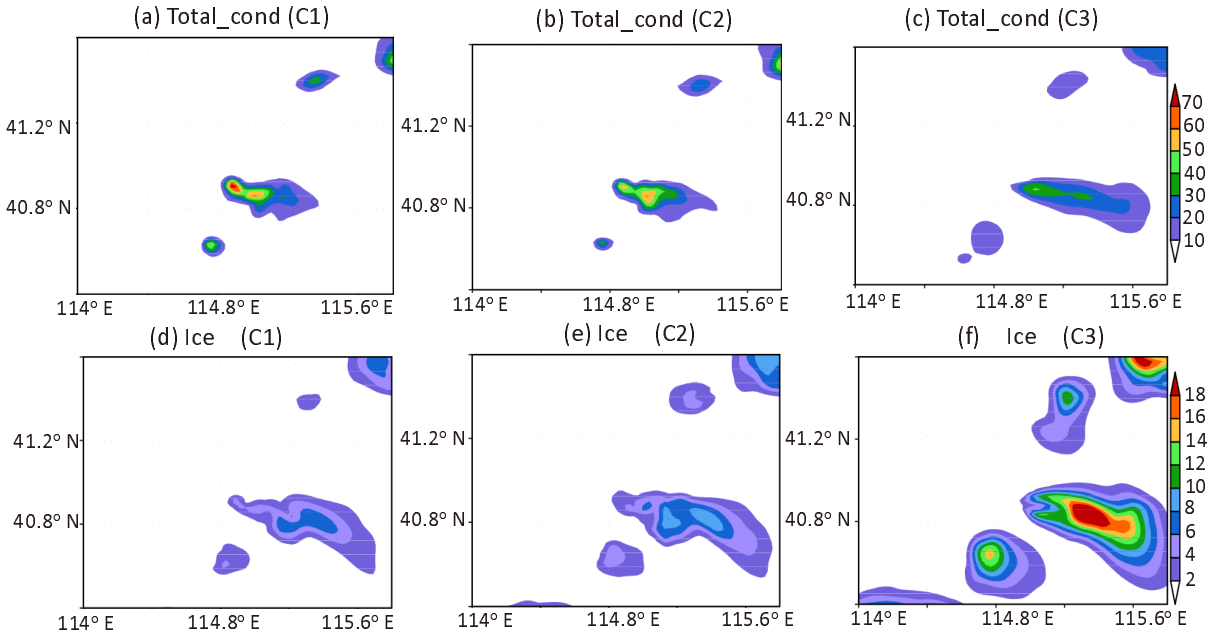

Fig. 4. Vertically integrated condensate mixing ratio and ice mixing ratio at 0700 UTC 23 July 2009 (SUM) for the three experiments (C1, C2, C3) (units: g kg^{-1}).

formula (for the hydrometeor mixing ratio) is

$$\text{vint} = \int_{p(x,y)}^{\text{top}} r(x,y,p)dp\ , \qquad (1)$$

where vint represents the integrated mixing ratio from the ground to the domain top; top is the pressure at the integral upper limit; $p(x,y)$ is the pressure at the ground point (x,y); and $r(x,y,p)$ represents the integral variables (e.g., total condensate mixing ratio, ice mixing ratio, etc.) at the ground point (x,y,p), where (x,y) are the longitude and latitude coordinates and p is the pressure (altitude).

Comparing the simulation results between the SPR case and SUM case, the total condensate mixing ratio maximum for the SUM case (Figs. 4a–c) is higher than that of the SPR case (Figs. 3a–c). In contrast, the maximum ice-phase mixing ratio for the SUM case (Figs. 4d–f) is smaller than that for the SPR case (Figs. 3d–f).

The anvil of clouds in the clean condition (C1) for the SPR case (Fig. 3a) covers a smaller area but achieve greater condensate mixing ratio maxima and is better organized than in the polluted (C2) and heavily polluted (C3) conditions

(Figs. 3b and c). The results indicate that an increase in the CCN concentration decreases the maxima of the total condensate mixing ratio but expands the spatial area of the cloud anvil. For the SUM case, we can obtain the same conclusion (Fig. 4). The numerous small-sized cloud droplets produced by CCN from aerosols can ascend to higher altitude in the atmosphere, and then freeze into small-sized ice particles with increasing CCN concentrations. On the one hand, the release of the latent heat of cloud droplets due to freezing at higher altitude further invigorates the outflow and leads to the formation of a larger convective cloud anvil. On the other hand, the small-sized ice crystals spread easily with the wind field. Therefore, according to this study, the anvil of clouds expands with enhancing CCN concentrations—a conclusion that differs from the findings of previous studies; for example, van den Heever et al. (2006) found that the cloud anvils of severe storms cover a smaller area and have larger condensate mixing ratio maxima under conditions of greater CCN concentrations. The differences between the present study and previous work illustrates that the impacts of aerosols on convective clouds vary on a regional basis, and thus more studies are needed that focus on different regions and seasons.

The ice-phase mixing ratio maxima under the clean condition (Fig. 3d for the SPR case; Fig. 4d for the SUM case) are smaller than those under the polluted and heavily polluted conditions (Figs. 3e and f for the SPR case; Figs. 4e and f for the SUM case), which indicates that an enhancement of the CCN concentration increases the ice-phase mixing ratio maximum. The effects of CCN on the total condensate mixing ratio and ice-phase mixing ratio possess similar trends of change for both the SPR and SUM cases.

The differences among the simulation results under the three CCN conditions (C1, C2, C3) might be caused by different mechanisms of CCN impacts on the formation of hydrometeor particles. Small cloud droplets, aggregates, rain droplets and hail account for the majority of all condensate amounts for the SPR and SUM cases (Figs. 5 and 6). When CCN concentrations increase, the mixing ratios of small cloud droplets and aggregates increase, but the diameters of these two hydrometeors diminish. Large numbers of small-sized particles spread out easily, following the wind field, in the upper layers of convective clouds under the polluted conditions. Hence, the anvil in the clean case is better organized than in the polluted case. Aggregates and hail account for the majority of ice-phase particles. The mixing ratio of aggregates increases, while the mixing ratio of hail particles decreases, with increasing CCN concentrations. The mixing ratio of aggregates is larger than that of hail particles for the SPR and SUM cases (Figs. 5 and 6). Therefore, higher CCN concentrations increase the ice-phase mixing ratio maxima in hailstorm clouds, for both the SPR and SUM cases.

4.2. *Effects of CCN on the vertical distributions of hydrometeor particles*

The primary hailfall area is area A for the SPR case (23 April 2009) and area B for the SUM case (23 July 2009) (see section 2). The vertical profiles of domain-averaged mixing ratios for all hydrometers within the convective updraft areas are shown in Figs. 5 and 6, corresponding to the SPR and SUM cases, respectively. The vertical profiles vary with CCN concentration.

Firstly, the effects of CCN on hydrometeor characteristics for the SPR case (Fig. 5) can be summarized as follows:

(1) Small cloud droplets (cloud1, Qc): The cloud water mixing ratios of small cloud droplets mainly appear below the height of 7 km. Maximum cloud water content is located at the heights of 5 km and 2 km, respectively. The mixing ratios of small cloud droplets above the freezing level (about 2.7 km) are much greater than those below the freezing level. At the freezing level, the mixing ratio of cloud water for small cloud droplets decreases significantly, with more hail particles produced in experiments C1 and C2 but more graupel particles in experiment C3. The results indicate that the accretion of small cloud droplets by hail is the main sink of small cloud droplets in C1 and C2, while the accretion of small cloud droplets by graupel is the main sink of small cloud droplets in C3. The reason for this difference is that enhancement of the CCN concentration can produce greater cloud water amounts of small cloud droplets at mid–high levels of convective cloud under polluted conditions, as compared with those under the clean condition. The cloud water offers plentiful amounts of supercooled water into the upper levels above the freezing level, which is favorable for the accretion growth of large-sized ice-phase hydrometeor particles. This conclusion is the same as in previous work (e.g., van den Heever et al., 2006).

(2) Large cloud droplets (Cloud2, Qc2): The cloud water mixing ratios of large cloud droplets are dependent on the activation of GCCN and the accretion of small cloud droplets. The Qc2 maxima under the C2 and C3 conditions appear at the height of 2 km below the freezing level. There are two peaks in C1, with a maximum value of 0.002 g kg^{-1} and 0.022 g kg^{-1} at the height of 2 km and 4.5 km, respectively. The Qc2 is much less under the polluted and heavily polluted conditions (C2, C3) compared with the clean condition (C1), indicating that higher CCN number concentrations reduce the accretion rate of large cloud droplets with small cloud droplets.

(3) Rain drops (Qr): Rainwater mainly appears in lower layers of the cloud (1.5–2 km), and graupel and hail mixing ratios decrease obviously at this level, which indicates the major sources of rainwater are the melting of graupel and hail. The mixing ratio of rainwater decreases, but the mean diameter of rain drops increases, with increasing CCN concentrations (the domain-averaged mean diameter for rain drops is 1.0 mm, 1.8 mm and 2.7 mm for C1, C2 and C3, respectively). Under the C1 condition, the rain droplets are smallest and it is therefore easier for them to be transported to higher altitudes by updrafts. Therefore, a small amount of supercooled rainwater appears above the freezing level under the C1 condition. However, under the C3 condition, a large number of small cloud droplets forms and the accretion rates of rainwater with cloud water weakens. This means that a large number of CCN inhibits the formation of rain drops.

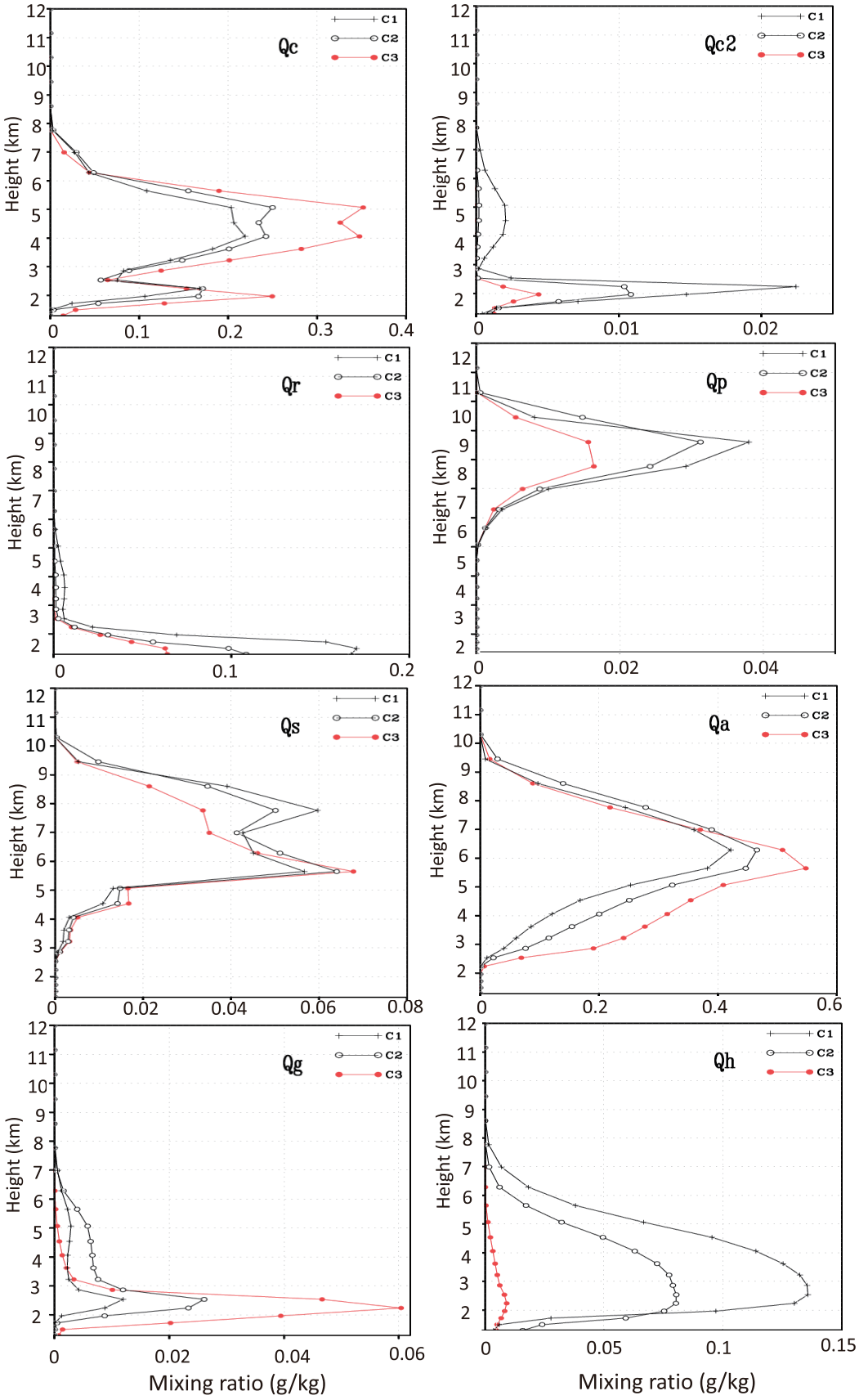

Fig. 5. Vertical profiles of the horizontally averaged hydrometeor mixing ratios at 0700 UTC 23 April 2009 (SPR) for the three sensitivity experiments (C1, C2, C3) (Q, mixing ratio; c, small cloud droplets; c_2, large cloud droplets; r, rain droplets; p, pristine ice crystals; s, snow; a, aggregates; g, graupel; h, hail.

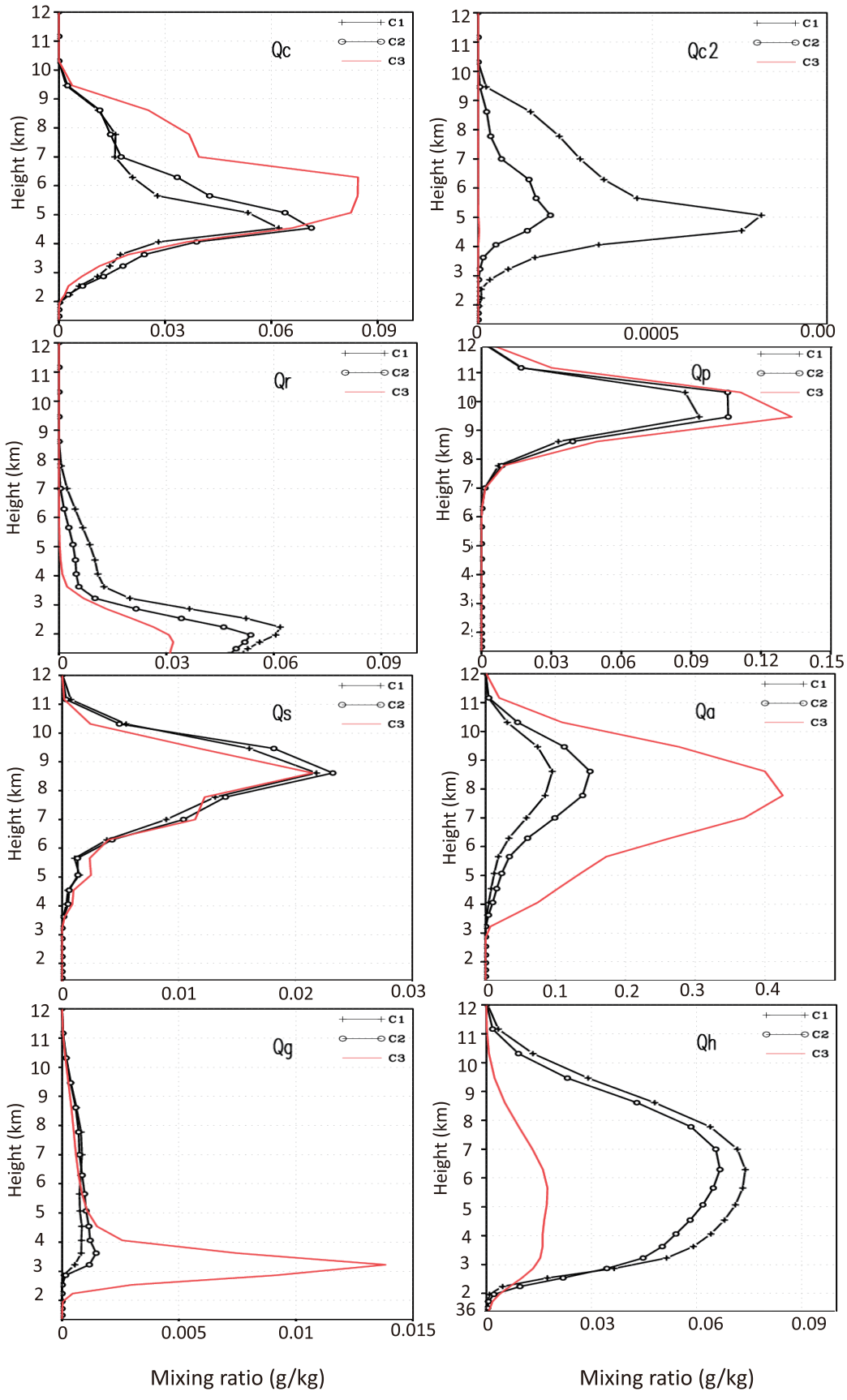

Fig. 6. Vertical profiles of the horizontally averaged hydrometeor mixing ratios at 0700 UTC 23 July 2009 (SUM) for the three sensitivity experiments (C1, C2, C3). The symbols are the same as those detailed in Fig. 5.

(4) Pristine ice (Qp): Pristine ice mainly appears at the height of 8.6 km (about −28°C). The mixing ratio of pristine ice decreases with increasing CCN concentrations. The activation of CCN requires vapor and supercooled water, but the vapor and supercooled water content are limited, meaning the CCN of higher number concentrations become large numbers of small cloud droplets. This increases the consumption of water vapor above the freezing level, especially in the middle levels (4–6 km), and prevents the water vapor from transporting further upwards, which is a disadvantage for the growth of pristine ice crystals. Therefore, an increasing concentration of CCN results in a decrease of the water mixing ratio of pristine ice crystals in higher level of the convective clouds.

(5) Snow (Qs): Snow is defined as larger pristine ice crystals (> 100 μm), which have grown by vapor deposition and riming. CCN affect the formation of pristine ice and then influenced the formation of snow. Two peaks of snow mixing ratio appear at the height of 5.7 km and 7.8 km, respectively. From the model results, at higher altitude (above 6 km), the main sources of snow are the autoconversion of pristine ice into snow. At lower altitude (below 6 km), the main sources of snow are the accretion of cloud water by pristine ice and the accretion of cloud water by snow. Above 6 km, the pristine ice mass is the least under the C3 condition, and therefore the snow generated by the autoconversion of pristine ice is the least. Below 6 km, the mixing ratio of small cloud droplets is the greatest under the C3 condition, which is beneficial for the accretion of cloud water by snow, and the mixing ratio of snow is greatest.

(6) Aggregates (Qa): Aggregates are the ice-phase particles formed by collision and coalescence among pristine ice, snow, and other aggregates. From Fig. 5, the peak aggregates mixing ratio appears at the height of 6.2 km; meanwhile, the snow at this height is obviously decreased, which indicates the main source of aggregates is the accretion of snow. Below 7 km, the snow is greatest under the C3 condition, which is beneficial for the accretion of snow by aggregates, and therefore the aggregates mixing ratio increases with increasing CCN concentrations. Above 7km height, the aggregates mixing ratio is greatest under the C2 condition.

(7) Graupel (Qg): Above the height of 3.5 km, the graupel mixing ratio is greatest in the C2 case. More graupel is produced under the C1 condition compared with that under the C3 condition. Below 3.5 km, an increasing CCN concentration results in more graupel in the cloud. In RAMS, graupel is defined as forming via moderate to heavy riming or partial melting of pristine ice, snow or aggregates. The mixing ratio of aggregates decreases obviously below 3.5 km in Fig. 5. Therefore, the increase in graupel with enhanced CCN concentrations is due to the increase in riming and subsequent melting processes of aggregates.

(8) Hail (Qh): When CCN concentrations increase, the hail mixing ratio decreases. The supercooled water benefits the growth of hail particles. The accretion of large droplets (cloud2 and rain) by hail takes place more easily than the collection of small cloud droplets (cloud1). Cloud2 and rain mixing ratios decrease with increasing CCN concentrations. The accretion of large droplets weakens with increasing CCN concentrations.

Comparing the simulations of hailstorms between the SUM case and the SPR case, some similar features are found for the relations between microphysical properties and various CCN number concentrations for the two seasonal hailstorms. It is interesting to note the differences of the hailstorms between the SUM case (Fig. 6) and the SPR case (Fig. 5) as follows:

The impacts of CCN number concentration on pristine ice for the SPR case differ from those for the SUM case. An increase in the CCN number concentration tends to reduce the pristine ice mixing ratio in the SPR case but enhance it in the SUM case. In the SPR case, the low-level water vapor is smaller than that in the SUM case. Higher CCN number concentrations enhance the competition for water vapor and supercooled water, generate more pristine ice particles but with smaller diameters, more evaporation, and therefore the pristine ice mixing ratio decreases with an increase in the CCN concentration. In the SUM case, more water vapor and supercooled water facilitates the growth of pristine ice particles, and the pristine ice mixing ratio increases with an enhancement in the CCN concentration.

In summary, an enhancement in the CCN concentration generally results in a greater amount of small cloud droplets, aggregates and graupel, but a smaller amount of large cloud droplets, rain drops, snow and hail. Increasing CCN concentrations produce greater differences for pristine ice mixing ratios between the SPR case and the SUM case.

4.3. *Impacts of CCN on hail particle characteristics*

The hail formation mechanism in severe hailstorms is one of the most important problems in cloud physics. The averaged hail properties (including mixing ratio, number concentration, and mean diameter) and the melting characteristics for the sensitivity experiments are shown in Table 1 for the SPR case, and in Table 2 for the SUM case. A study for the SPR case has been conducted before (Yang et al., 2011).

The SPR and SUM hailstorm cases possess some similar features under different aerosol conditions. The hailstorm clouds under clean conditions (C1) have the largest mixing ratio ($\overline{Q_h}$) and number concentration ($\overline{N_h}$) of hail in clouds, while the hailstorm clouds under the polluted conditions (C2) are characterized by maximum values near the ground. Under the heavily polluted conditions (C3), the hailstorm has the lowest values in clouds, as well as near the ground. The hailstorm cloud under polluted conditions (C2) has a larger hailfall amount than under clean conditions (C1) and heavily polluted conditions (C3), and the reason is that the melting amount under the C2 condition (33.4×10^{-3} g kg^{-1}) is less than that under the C1 condition (43.3×10^{-3} g kg^{-1}).

There are also some differences between the SPR and SUM cases. The melting amounts in clouds are far less than those under the cloud base in the SPR cases (C1, C2, C3), while the melting amounts in clouds are greater compared with those under the cloud base in the SUM cases (C1, C2). This is due to a deeper warm cloud layer in the SUM cases

Table 1. Domain-averaged (area A) and time-averaged (0550–0930 UTC) quantities for hail particles in the SPR cases.

	IN/SURF			IN/OUT
Experiment	$\overline{Q_h}$ (10^{-2} g kg^{-1})	$\overline{N_h}$ (m^{-3})	$\overline{D_h}$ (mm)	$\overline{Q_{melt}}$ (10^{-3} g kg^{-1})
C1	3.1/1.4	25.0/3.2	6.1/6.7	1.9/30.0
C2	1.6/1.9	7.1/3.2	6.4/7.1	1.0/21.6
C3	0.1/0.8	0.2/1.0	8.9/7.9	0.3/4.5

Notes: $\overline{Q_h}$, hail mixing ratio; $\overline{N_h}$, hail concentration; $\overline{D_h}$, hail mean diameter; $\overline{Q_{melt}}$, melting mixing ratio; the horizontal line above the variable means average variable. IN, hydrometeor characteristics in cloud; SURF, hydrometeor characteristics at the point where they reach the surface of the earth; OUT, hydrometeor characteristics between the surface of the earth and the cloud-base height.

Table 2. Domain-averaged (area B) and time-averaged (0520–0930 UTC) quantities for hail particles in the SUM cases.

	IN/SURF			IN/OUT
Experiment	$\overline{Q_h}$ (10^{-2} g kg^{-1})	$\overline{N_h}$ (m^{-3})	$\overline{D_h}$ (mm)	$\overline{Q_{melt}}$ (10^{-3} g kg^{-1})
C1	$33.3\times10^{-1}/4.24\times10^{-1}$	$134.6\times10^{-1}/1.87\times10^{-1}$	6.00/5.011	22.1/10.1
C2	$31.0\times10^{-1}/4.33\times10^{-1}$	$75.0\times10^{-1}/1.64\times10^{-1}$	6.15/5.024	20.4/9.49
C3	$14.0\times10^{-1}/3.7\times10^{-1}$	$5.08\times10^{-1}/0.85\times10^{-1}$	7.63/5.15	6.56/11.6

Note: symbols/abbreviations are the same as in Table 1.

than that in the SPR cases. Based on the sounding data at Zhangjiakou, close to the scene of the hailstorms concerned, the height of the melting level for the SUM cases at 0000 UTC 23 July 2009 is 4.4 km, while the height of the melting level for the SPR cases at 0000 UTC 23 April 2009 is 2.7 km. This is due to the increase in the thickness of the warm cloud layer for the SUM cases (4.4 km) compared with that for the SPR cases (2.7 km).

4.4. *Influences of aerosol on hail microphysical processes*

Hail grows by accreting with cloud water, rainwater, pristine ice, snow, aggregates, and graupel particles. Tables 3 and 4 present the contributions of the domain-3 (G3)–integrated and time-averaged value of each hydrometeor particle type to the total hail water content in the three aerosol experiments (C1, C2, C3) for the SPR case and SUM case, respectively. They can be used to analyze the main source of hail growth.

Table 3 lists the transfer amount (units: g kg^{-1}) of each hydrometeor particle type in the cloud, averaged over time (0550–0930 UTC) in area A, to hail, in the three experiments for the SPR case. The values of C_{cld1} (C_{cld2}, C_r, C_i, C_s, C_a, and C_g) signify the relative contributions of cloud1 droplets (cloud2 droplets, rain drops, pristine ice, snow, aggregates, and graupel) to hail growth, which is achieved by the accretion of other hydrometeor particles (i.e., cloud1 droplets, cloud2 droplets, rain drops, pristine ice, snow, aggregates, and graupel) by hail. The hailstorm in the SPR case has been studied before (Yang et al., 2011, Table 3), and therefore will not be covered again here.

The hailstorm in the SUM case is the focus in the following text. Table 4 shows that cloud1 is the largest contributor to hail. The relative contribution rate of cloud1 to hail in C1, C2 and C3 is 58.4%, 63.6% and 60.3%, respectively. Rain is the second largest contributor to hail. The contribution rate of rain to hail in C1, C2 and C3 is 32.5%, 26.4% and 24.8%, respectively. This indicates that the contribution rates of rain to hail decrease with increasing CCN concentration. Aggregates are the third largest contributor to hail. The contribution rate of aggregates to hail in C1, C2 and C3 is 4.3%, 6.2% and 10.4%, respectively, which illustrates that the contribution rate of aggregates to hail enhances with an increase in CCN concentration.

The contribution rates of total supercooled liquid water (i.e., cloud1, cloud2 and rain) to hail in C1, C2 and C3 is 92.5%, 90.2% and 85.1%, respectively. Meanwhile, the contribution rate of ice-phase hydrometeors (i.e., aggregates, graupel, pristine ice and snow) to hail in C1, C2 and C3 is 7.5%, 9.8% and 14.9%, respectively. Therefore, the contribution of liquid water to hail decreases, while the contribution of ice-phase particles to hail increases, with an enhanced CCN concentration.

A similarity between the SPR and SUM case is that cloud1 makes the largest contribution to hail growth. However, there are also some differences. In the SPR case, the contributions of aggregates and graupel to hail are greater than the contribution of rain to hail. Whereas, in the SUM case, the contributions of aggregates and graupel to hail are less than the contribution of rain to hail. Compared with the SPR case, liquid water makes more of a contribution to hail generation in the SUM cases. This is due to a deeper warm cloud layer in the SUM case than that in the SPR case.

4.5. *Effects of CCN on the horizontal distribution of precipitation rate*

Another aspect associated with convective storms that is affected by the variation in aerosol concentrations is the distribution of the surface precipitation rate. Figure 7 shows the horizontal distribution of the rain and hail precipitation rates at 0700 UTC for the SPR case under the three different CCN conditions (C1, C2 and C3). As can be seen, an

Table 3. Transfer amount (g kg^{-1}) of each hydrometeor particle type in the cloud, averaged over time (0550–0930 UTC) in area A, to hail, in the three experiments for the SPR case.

Experiment	C_c	C_{c2} (10^{-2})	C_r	C_i (10^{-5})	C_s (10^{-2})	C_a	C_g	Total
C1	19.7	67	2.68	358	138	9.0	2.72	36.15
C2	11.2	11	1.68	67.8	69	8.7	3.89	26.27
C3	1.25	0.52	1.72	5.41	2.37	2.15	0.79	8.29

Notes: C, transfer amount (g kg^{-1}) of each particle to hail; subscript "c", cloud1; subscript "c2", cloud2; subscript "r", raindrop; subscript "i", ice crystal; subscript "s", snow; subscript "a", aggregate; subscript "g", graupel; Total = $C_a + C_{cld1} + C_{cld2} + C_g + C_i + C_r + C_s$.

Table 4. Transfer amount (g kg^{-1}) of each particle in the cloud, averaged over time (0520–0930 UTC) in area B, to hail, in the three experiments for the SUM case.

Experiment	C_c	C_{c2} (10^{-2})	C_r	C_i (10^{-5})	C_s (10^{-2})	C_a	C_g	Total
C1	35.3	94	19.6	951	121	2.6	0.65	60.4
C2	33.2	15.1	13.8	845	101	3.22	0.78	52.3
C3	10.7	0.07	4.41	170	8.51	1.85	0.69	17.8

Note: symbols are the same as in Table 3.

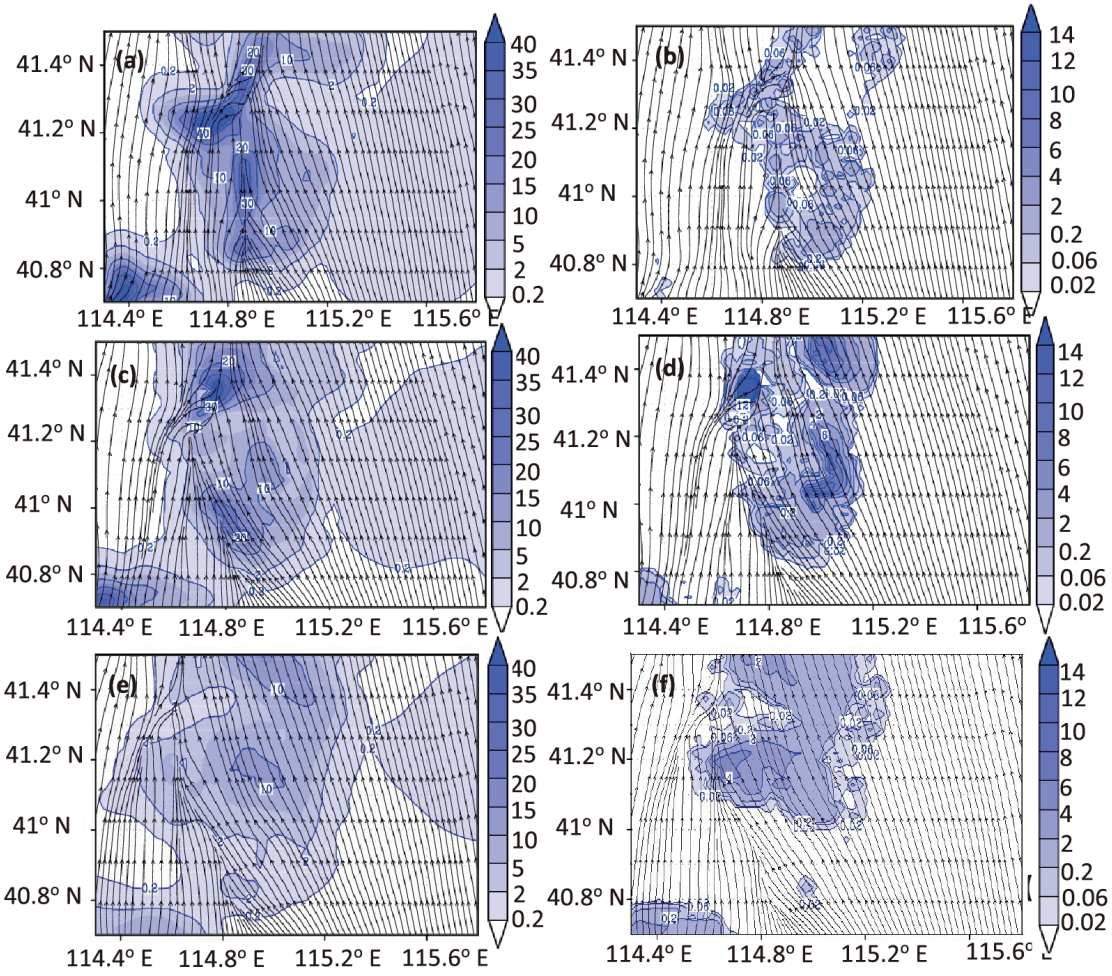

Fig. 7. The horizontal distribution of rain [(a) C1; (b) C2; (e) C3] and hail [(b) C1; (d) C2; (f) C3] precipitation (units: mm h^{-1}) at 0700 UTC for the SPR case. The stream lines are the surface wind field.

increasing CCN concentration reduces the amount and area of the surface rainfall rate (Figs. 7a, c and e). The hailfall rate is greatest under the polluted (C2) condition among the three experiments (Figs. 7b, d and f). It is demonstrated that a moderate increase in the CCN concentration is beneficial to hailfall, while overly high or low CCN concentrations are not conducive to hail precipitation.

In the SUM case, the rainfall rate is greatest under the clean (C1) condition (Figs. 8a, c and e), while the hail precipitation rate is greatest under the seriously polluted (C3) condition among the three experiments (Figs. 8b, d and f), which indicates that an increasing CCN concentration reduces the surface rainfall rate but enhances the hailfall rate.

The largest difference between the SPR and SUM cases relates to the hailfall under the seriously polluted (C3) condition. The hailfall rate is lowest under C3 in the SPR case, but highest under C3 in the SUM case. It is evident that an increasing CCN concentration has different effects on the hailfall rate in different seasons.

4.6. *Influences of CCN on accumulated precipitation*

Tables 5 and 6 show the total accumulated precipitation and ice-phase precipitation for the SPR case (area A, 0550–0930 UTC) and the SUM case (area B, 0520–0930 UTC). For the SPR case (Table 5), the total precipitation amount (TPA) under the clean condition (C1) is the greatest among the three experiments, which illustrates that large CCN concentrations

Table 5. TPA and IPA (area A, 0550–0930 UTC) for the three sensitivity tests in the SPR case.

Experiment	TPA (10^{13} kg)	TPR (%)	IPA (10^{13} kg)/ RC (%)	IPR (%)
C1	50.5	—	2.17/4.32	—
C2	38.7	−23.4	7.48/19.33	+243
C3	24.4	−51.7	6.39/26.19	+193

Notes: TPR, TPA rate of change compared with C1; IPR, IPA rate of change compared with C1.

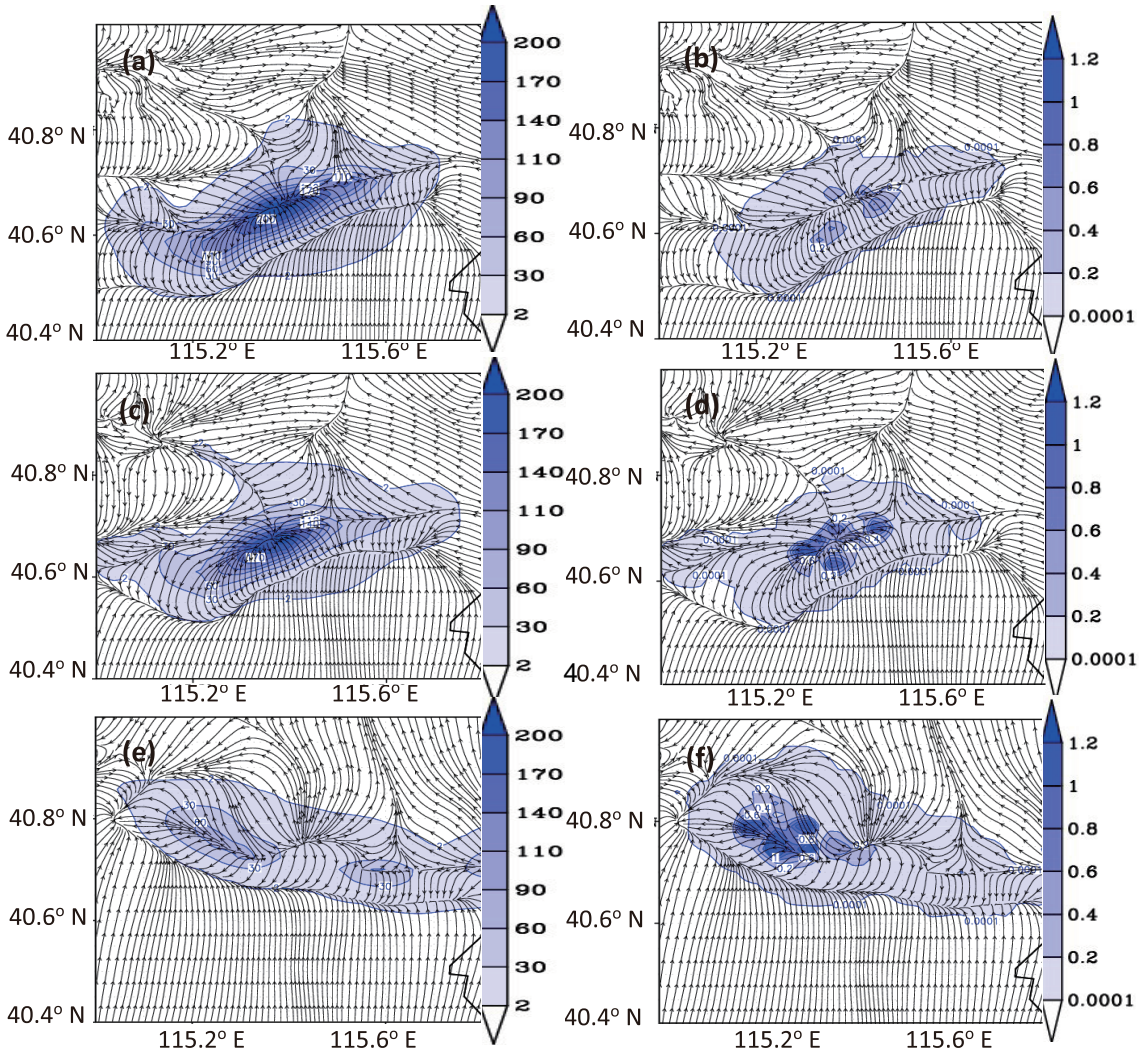

Fig. 8. The horizontal distribution of rain [(a) C1; (c) C2; (e) C3] and hail [(b) C1; (d) C2; (f) C3] precipitation (units: mm h^{-1}) at 0700 UTC for the SUM case. The stream lines are the surface wind field.

Table 6. TPA and IPA (area B, 0520–0930 UTC) for the three sensitivity tests in the SUM case.

Experiment	TPA (10^{13} kg)	TPR (%)	IPA (10^{13} kg)	IPR (%)
C1	78.5	—	2.32×10^{-2}	—
C2	72.2	−8.0	4.17×10^{-2}	79.7
C3	44.8	−42.9	14.5×10^{-2}	247.7

Note: abbreviations are the same as in Table 5.

are linked to the TPA decreasing. The ice-phase precipitation amount (IPA) under the polluted condition (C2) is maximal, while its relative contribution (RC) ratio to the TPA intensifies as the CCN concentration increases. The difference between the SPR case and the SUM case is the variation in ice-phase precipitation with increasing CCN concentration.

In summary, for the two seasonal hailstorm cases analyzed in this study, the season variation has some effects on surface precipitation. The similarities are: the total surface precipitation amount decreases with an enhancement in CCN, while the RC ratio of the IPA to the TPA enhances with an increasing CCN concentration. The differences are: the IPA increases with an enhancement in CCN in the SUM case; however, the ice-phase precipitation amount is greatest under C2 for the spring case.

5. Conclusions

The present study uses the RAMS model to simulate two severe hailstorms that occurred in spring (SPR) and summer (SUM), respectively, in a semiarid region of northern China. The differences and similarities of the CCN effects between the SPR hailstorm and SUM hailstorm in the semiarid region are investigated. Figure 9 and Table 7 illustrate the train of thought for this study. The CCN number concentrations for polluted clouds in our study are much higher than in previous studies. Our simulations demonstrate that many characteristics of both the hydrometer particle properties, hail formation mechanisms, and anvil stages of storm development, are sensitive to changes in the CCN concentration. The analyses show that the primary similarities of these effects on the two hailstorms are as follows:

(1) Enhancement of the CCN concentration results in producing greater amounts of small cloud droplet, snow crystal, aggregate and graupel water content, but lesser amounts of large cloud droplet, rain drop and hail water content. High CCN concentrations produce large differences in the water content of pristine ice crystals in both hailstorms.

(2) The total hydrometeor mixing ratio decreases, while the total ice-phase mixing ratio enhances, with increasing CCN concentration. Meanwhile, the area covered by the cloud anvil is extended when the CCN concentration in-

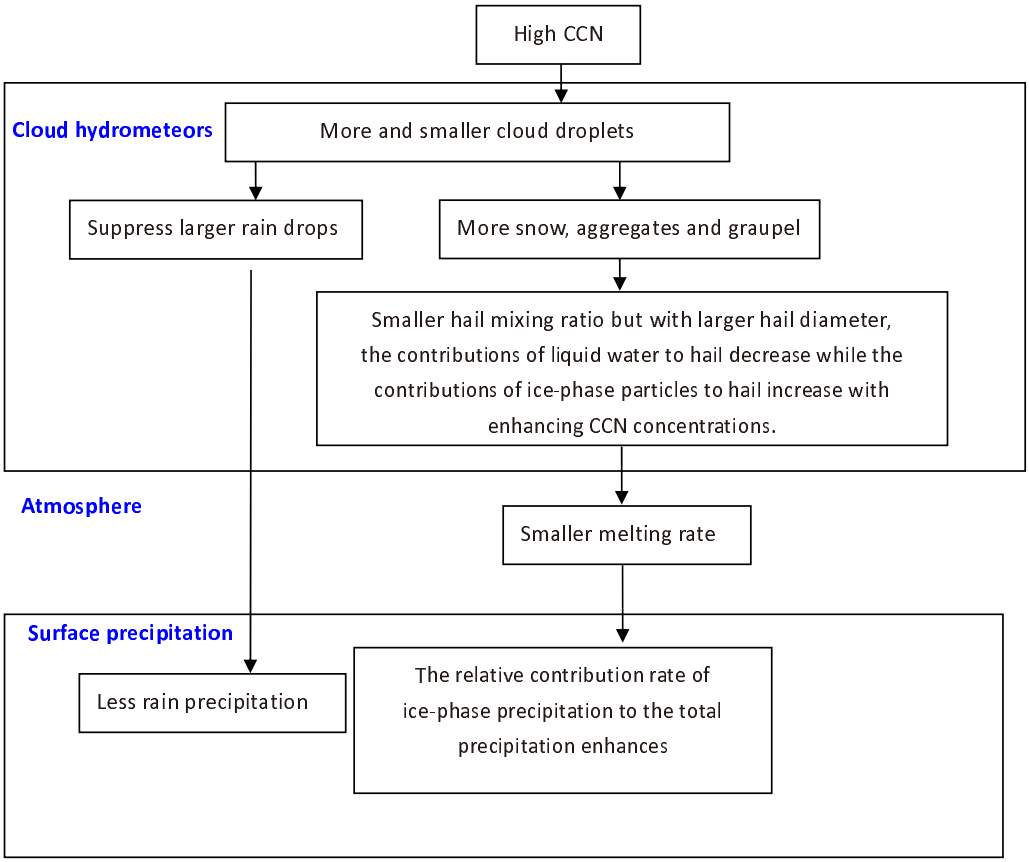

Fig. 9. Illustration of the train of thought in the present study: the similar effects of CCN on the two seasonal hailstorm cases.

Table 7. The different effects of CCN concentration on the two seasonal hailstorms.

	SPR cases	SUM cases
Microphysical properties	Less pristine ice with high CCN concentration	More pristine ice with high CCN concentration
Melting properties	Melting amount in clouds less than that under the cloud base	Melting amount in clouds greater than that under the cloud base
Hail particle properties	Contributions of aggregates and graupel to hail greater than the contribution of rain to hail	Contributions of aggregates and graupel to hail less than the contribution of rain to hail
Hailfall properties	Hail precipitation greatest in the polluted clouds (C2)	Hail precipitation greatest in the seriously polluted clouds (C3)

creases.

(3) As the CCN concentration increases, the supercooled cloud water and rainwater provide a lesser contribution to hail, while the ice-phase hydrometeors play an active role in the development of hail.

(4) When the CCN concentration increases, the total surface precipitation amount, surface rainfall amount and rainfall area all reduce, while the RC ratio of the IPA to TPA enhances.

On the other hand, the main differences between the two hailstorms can help us to understand the impacts of aerosols on hailstorms in the different environments of two different seasons. Some meaningful conclusions can be made as follows:

(1) An increase in the CCN concentration tends to reduce the pristine ice mixing ratio in the SPR case, but enhance it in the SUM case.

(2) Ice-phase hydrometeor particles provide a greater contribution to hail growth in the SPR hailstorm case, while liquid water contributes more in the SUM hailstorm case.

(3) An increasing CCN concentration also has different effects on surface hail precipitation in the two different hailstorm cases, i.e., in different seasons. Hailfall is lowest under the seriously polluted condition (C3) in the SPR case, while it is greatest under the same condition in the SUM case. It is interesting to note that hail precipitation shows a clearly monotonic behavior when the environment is relatively more polluted in terms of aerosols.

Given that the impact of aerosols on severe convective clouds is complex and varies both seasonally and regionally, the results presented here on the differences and similarities of CCN effects on hailstorms in different seasons are only representative of the two cases studied. Therefore, more and deeper investigations on this issue are needed in the future for different climatic regions and seasons.

Acknowledgements. This work was partially supported by the National Natural Science Foundation of China (Grant Nos. 41205099 and 41575037), the National Grand Fundamental Research 973 Programs of China (Grant Nos. 2014CB441403 and 2013CB430105), the Special Scientific Research Project of the Meteorological Public Welfare Profession of China (Grant No. GYHY201006031), the Guizhou Province Scientific Research Joint Project (Grant No. G[2013]4001), and the National Science Foundation of China (Grant No. 41405128). The authors also wish to thank Dr. Stephen M. SALEEBY of Colorado State University for providing the RAMS code.

REFERENCES

Albrecht, B., 1989: Aerosols, cloud microphysics, and fractional cloudiness. *Science*, **245**(4923), 1227–1230.

Andreae, M. O., D. Rosenfeld, P. Artaxo, A. A. Costa, G. P. Frank, K. M. Longo, and M. A. F. Silva-Dias, 2004: Smoking rain clouds over the Amazon. *Science*, **303**(5662), 1337–1342.

Borys, R. D., D. H. Lowenthal, and D. L. Mitchell, 2000: The relationships among cloud microphysics, chemistry, and precipitation rate in cold mountain clouds. *Atmos. Environ.*, **34**, 2593–2602.

Chen, B. J., and H. Xiao, 2010: Silver iodide seeding impact on the microphysics and dynamics of convective clouds in the high plains. *Atmospheric Research*, **96**, 186–207.

Chen, B. J., W. Hu, and J. P. Pu, 2011a: Characteristics of the raindrop size distribution for freezing precipitation observed in southern China. *J. Geophys. Res.*, **116**, D06201, doi: 10.1029/2010JD015305.

Chen, Q., Y. Yin, L. J. Jin, H. Xiao, and S. C. Zhu, 2011b: The effect of aerosol layers on convective cloud microphysics and precipitation. *Atmospheric Research*, **101**, 327–340.

Cheng, W. Y. Y., G. G. Carrió, W. R. Cotton, and S. M. Saleeby, 2009: Influence of cloud condensation and giant cloud condensation nuclei on the development of precipitating trade wind cumuli in a large eddy simulation. *J. Geophys. Res.*, **114**(D8), D08201.

Cotton, W. R., R. A. Pielke, R.L. Walko, G.E. Liston, C. J. Tremback, and H. L. Jiang, 2003: RAMS 2001: Current status and future directions. *Meteor. Atmos. Phys.*, **82**, 5–29.

Duan, Y., Z. H. Wu, L. X. Shi, and J. Yan, 2008: The primary study on distribution characteristics of aerosols and CCN under clear sky weather condition in summer using aircraft detection over the Bohai Sea gulf area, China. *Proceedings of the 15th International Conference on Clouds and Precipitation*, Cancun, Mexico.

Feingold, G., B. Stevens, W. R. Cotton, and R. L. Walko, 1994: An explicit cloud microphysics/LES model designed to simulate the Twomey effect. *Atmospheric Research*, **33**, 207–233.

Feingold, G., W. R. Cotton, S. M. Kreidenweis, and J. T. Davis, 1999: The impact of giant cloud condensation nuclei on drizzle formation in stratocumulus: Implications for cloud radiative properties. *J. Atmos. Sci*, **56**(24), 4100–4117.

Flossmann, A. I., and W. Wobrock, 2010: A review of our understanding of the aerosol-cloud interaction from the perspective of a bin resolved cloud scale modelling. *Atmospheric Research*, **97**, 478–497.

Guo, C.-W., H. Xiao, H.-L. Yang, and Q. Tang, 2014: Simulation of the microphysical processes and effect of latent heat on a heavy rainfall event in Beijing. *Atmospheric and Oceanic Science Letters*, **7**(6), 521–526.

Guo, C.-W., H., Xiao, H. L. Yang, and Q. Tang, 2015: Observation and modeling analyses of the macro- and microphysical characteristics of a heavy rain storm in Beijing. *Atmospheric Research*, **156**, 125–141.

Guo, X. L., D. H. Fu, and J. Wang, 2006a: Mesoscale convective precipitation system modified by urbanization in Beijing City. *Atmospheric Research*, **82**, 112–126.

Guo, X. L., G. G. Zheng, and D. Z. Jin, 2006b: A numerical comparison study of cloud seeding by silver iodide and liquid carbon dioxide. *Atmospheric Research*, **79**, 183–226.

Harrington, J. Y., M. P. Meyers, R. L. Walko, and W. R. Cotton, 1995: Parameterization of ice crystal conversion processes due to vapor deposition for mesoscale models using double-moment basis functions. Part I: Basic formulation and parcel model results. *J. Atmos. Sci.*, **52**(23), 4344–4366.

Hindman, E. E., M. A. Campbell, and R. D. Borys, 1994: A ten-winter record of cloud-droplet physical and chemical properties at a mountaintop site in Colorado. *J. Appl. Meteor.*, **33**, 797–807.

IPCC, 2007: Climate Change 2007: *The Physical Science Basis. Contribution of Working Group I to the Fourth Assessment Report of the Intergovernmental Panel on Climate Change*, Solomon et al., Eds., Cambridge University Press, Cambridge, United Kingdom and New York, NY, USA, 996 pp.

Kaufman, Y. J., and T. Nakajima, 1993: Effect of Amazon smoke on cloud microphysics and albedo-analysis from satellite imagery. *J. Appl. Meteor.*, **32**(4), 729–744.

Kaufman, Y. J., I. Koren, L. A. Remer, D. Rosenfeld, and Y. Rudich, 2005: The effect of smoke, dust, and pollution aerosol on shallow cloud development over the Atlantic Ocean. *Proceedings of the National Academy of Sciences of the United States of America*, **102**(32), 11 207–11 212.

Khain, A., A. Pokrovsky, and I. Sednev, 1999: Some effects of cloud-aerosol interaction on cloud microphysics structure and precipitation formation: Numerical experiments with a spectral microphysics cloud ensemble model. *Atmospheric Research*, **52**(3), 195–220.

Khain, A., A. Pokrovsky, M. Pinsky, A. Seifert, and V. Phillips, 2004: Simulation of effects of atmospheric aerosols on deep turbulent convective clouds using a spectral microphysics mixed-phase cumulus cloud model. Part I: Model description and possible applications. *J. Atmos. Sci.*, **61**(24), 2963–2982.

Khain, A., D. Rosenfeld, and A. Pokrovsky, 2005: Aerosol impact on the dynamics and microphysics of deep convective clouds. *Quart. J. Roy. Meteor. Soc.*, **131**(611), 2639–2663.

Khain, A. P., D. Rosenfeld, and A. Pokrovsky, 2001: Simulating convective clouds with sustained supercooled liquid water down to −37.5°C using a spectral microphysics model. *Geophys. Res. Lett.*, **28**(20), 3887–3890.

Koren, I., Y. J. Kaufman, D. Rosenfeld, L. A. Remer, and Y. Rudich, 2005: Aerosol invigoration and restructuring of Atlantic convective clouds. *Geophys. Res. Lett.*, **32**, L14828, doi: 10.1029/2005GL023187.

Lin, J. C., T. Matsui, R. A. Pielke Sr., and C. Kummerow, 2006: Effects of biomass-burning-derived aerosols on precipitation and clouds in the Amazon Basin: A satellite-based empirical study. *J. Geophys. Res.*, **111**(D19), D19204.

Liu, X. L., and S. J. Niu, 2009: Numerical simulation on the evolution of cloud particles in 3-D convective cloud. *Science in China Series D: Earth Sciences*, **52**, 1195–1206.

Lynn, B. H., A. P. Khain, J. Dudhia, D. Rosenfeld, A. Pokrovsky, and A. Seifert, 2005: Spectral (bin) microphysics coupled with a mesoscale model (MM5). Part II: Simulation of a CaPE rain event with a squall line. *Mon. Wea. Rev.*, **133**(1), 59–71.

Mather, G. K., 1991: Coalescence enhancement in large multicell storms caused by the emissions from a Kraft paper mill. *J. Appl. Meteor.*, **30**(8), 1134–1146.

Meyers, M. P., P. J. DeMott, and W. R. Cotton, 1992: New primary ice-nucleation parameterizations in an explicit cloud model. *J. Appl. Meteor.*, **31**, 708–721.

Meyers, M.P., R.L. Walko, J.Y. Harrington, and W. R. Cotton, 1997: New RAMS cloud microphysics prameterization. Part II: The two-moment scheme. *Atmospheric Research*, **45**, 3–39.

Ohashi, Y., and H. Kida, 2002: Local circulations developed in the vicinity of both coastal and inland urban areas: A numerical study with a mesoscale atmospheric model. *J. Appl. Meteor.*, **41**, 30–45.

Phillips, V. T. J., T. W. Choularton, A. M. Blyth, and J. Latham, 2002: The influence of aerosol concentrations on the glaciation and precipitation of a cumulus cloud. *Quart. J. Royal. Meteor. Soc.*, **128**(581), 951–971.

Pitter, R. L., and H. R. Pruppacher, 1974: A numerical investigation of collision efficiencies of simple ice plates colliding with supercooled water drops. *J. Atmos. Sci.*, **31**, 551–559.

Rosenfeld, D., and I. M. Lensky, 1998: Satellite-based insights into precipitation formation processes in continental and maritime convective clouds. *Bull. Amer. Meteor. Soc.*, **79**(11), 2457–2476.

Rosenfeld, D., 2000: Suppression of rain and snow by urban and industrial air pollution. *Science*, **287**(5459), 1793–1796.

Rosenfeld, D., W. L. Woodley, T. W. Krauss, and V. Makitov, 2006: Aircraft microphysical documentation from cloud base to anvils of hailstorm feeder clouds in Argentina. *J. Appl. Meteor.*, **45**(9), 1261–1281.

Rosenfeld, D., U. Lohmann, G. B. Raga, C. D. O'Dowd, M. Kulmala, S. Fuzzi, A. Reissell, and M. O. Andreae, 2008: Flood or drought: How do aerosols affect precipitation. *Science*, **321**, 1309–1313.

Saleeby, S. M., and W. R. Cotton, 2004: A large-droplet mode and prognostic number concentration of cloud droplets in the Colorado State University Regional Atmospheric Modeling System (RAMS). Part I: Module descriptions and supercell test simulations. *J. Appl. Meteor.*, **43**(1), 182–195.

Saleeby, S. M., and W. R. Cotton, 2005: A large-droplet mode and prognostic number concentration of cloud droplets in the Colorado State University regional atmospheric modeling system (RAMS). Part II: Sensitivity to a Colorado Winter Snowfall Event. *J. Appl. Meteor.*, **44**, 1912–1929.

Saleeby, S. M., W. R. Cotton, D. Lowenthal, R. D. Borys, and M. A. Wetzel, 2009: Influence of Cloud Condensation Nuclei on orographic snowfall. *Journal of Applied Meteorology and Climatology*, **48**(5), 903–922.

Seifert, A., and K. D. Beheng, 2006: A two-moment cloud microphysics parameterization for mixed-phase clouds. Part 2: Maritime vs. continental deep convective storms. *Meteor. Atmos. Phys.*, **92**, 67–82.

Seifert, A., C. Köhler, and K. D. Beheng, 2012: Aerosol-cloud-precipitation effects over Germany as simulated by a convective-scale numerical weather prediction model. *Atmo-*

spheric Chemistry and Physics, **12**, 709–725.

Seigel, R. B., and S. C. van den Heever, 2013: Squall-line intensification via hydrometeor recirculation. *J. Atmos. Sci.*, **70**(7), 2012–2031.

Shepherd, J. M., and S. J. Burian, 2003: Detection of urban-induced rainfall anomalies in a major coastal city. *Earth Interactions*, **7**, doi: 10.1175/1087-3562(2003)007<0001:DOUIRA>2.0.CO;2.

Shi, L. X., and Y. Duan, 2007: Observations of cloud condensation nuclei in north China. *Acta Meteorologica Sinica*, **22**, 97–106.

Shi, Z., Y. B. Tan, H. Q. Tang, J. Sun, Y. Yang, L. Peng, and X. F. Guo, 2015: Aerosol effect on the land-ocean contrast in thunderstorm electrification and lightning frequency. *Atmospheric Research*, **164–165**, 131–141.

Squires, P., and T. Twomey, 1961: The relation between cloud drop numbers and the spectrum of cloud nuclei. *Physics of Precipitation, Monograph*, H. Weickmann, Ed., American Geophysical Union, 211–219.

Teller, A., and Z. Levin, 2006: The effects of aerosols on precipitation and dimensions of subtropical clouds: A sensitivity study using a numerical cloud model. *Atmospheric Chemistry and Physics*, **6**(1), 67–80.

Twomey, S., 1977: The influence of pollution on the shortwave albedo of clouds. *J. Atmos. Sci.* **34**(7), 1149–1152.

van den Heever, S. C., G. G. Carrió, W. R. Cotton, P. J. DeMott, and A. J. Prenni, 2006: Impacts of nucleating aerosol on Florida storms. Part I: Mesoscale simulations. *J. Atmos. Sci.*, **63**(7), 1752–1775.

Wang, P. K., and W. S. Ji, 2000: Collision efficiencies of ice crystals at low-intermediate Reynolds numbers colliding with supercooled cloud droplets: A numerical study. *J. Atmos. Sci.*, **57**, 1001–1009.

Xiao, H., H. Y. Xu, and M. Y. Huang, 1988: The study of numerical simulation on the formation of the cloud droplet spectra in cumulus Clouds-Part I: The roles of the spectra and concentrations of salt nuclei. *Scientia Atmospherica Sinica*, **12**(2), 143–157. (in Chinese with English abstract)

Xiao, H., Y. Yin, L. J. Jin, Q. Chen, and J. H. Chen, 2014: Simulation of aerosol effects on orographic clouds and precipitation using WRF model with a detailed bin microphysics scheme. *Atmospheric Science Letters*, **15**, 134–139.

Xiao, H., Y. Yin, Q. Chen, and P. G. Zhao, 2016: Impact of aerosol and freezing level on orographic clouds: A sensitivity study. *Atmospheric Research*, **176-177**, 19–28.

Yang, H. L., H. Xiao, and Y. C. Hong, 2011: A numerical study of aerosol effects on cloud microphysical processes of hailstorm clouds. *Atmospheric Research*, **102**, 432–443.

Yang, H. L., H. Xiao, and Y. C. Hong, 2012: The effects of giant cloud condensation nuclei on the structure of precipitation in hailstorm clouds. *Science China Earth Sciences*, **55**, 126–142.

Yang, H.-L., H. Xiao, and C.-W. Guo, 2015a: Structure and evolution of a squall line in northern China: A case study. *Atmospheric Research*, **158-159**, 139–157.

Yang, H.-L., H. Xiao, and C.-W. Guo, 2015b: Impacts of two ice parameterization schemes on the cloud microphysical processes and precipitation of a severe Storm in northern China. *Atmospheric and Oceanic Science Letters*, **8**(5), 301–307.

Yin, Y., Z. Levin, T. G. Reisin, and S. Tzivion, 2000a: The effects of giant cloud condensation nuclei on the development of precipitation in convective clouds-a numerical study. *Atmospheric Research*, **53**, 91–116.

Yin, Y., Z. Levin, T. Reisin, and S. Tzivion, 2000b: Seeding convective clouds with hygroscopic flares: Numerical simulations using a cloud model with detailed microphysics. *J. Appl. Meteor.*, **39**(9), 1460–1472.

Yin, Y., K. S. Carslaw, and G. Feingold, 2005: Vertical transport and processing of aerosols in a mixed-phase convective cloud and the feedback on cloud development. *Quart. J. Roy. Meteor. Soc.*, **131**(605), 221–245.

Zhao, C. S., Y. Ishizaka, and D. Y. Peng, 2005: Numerical study on impacts of multi-component aerosols on marine cloud microphysical properties. *J. Meteor. Soc. Japan*, **83**, 977–986.